A Bayesian framework for estimating uncertainty in long-term solar forcing

Ted Amdur and Peter Huybers

This work is supported by Future Investigators in NASA Earth and Space Science and Technology (FINESST-19) grant 80NSSC19K1327

The Frozen Thames (Abraham Hondius 1677)

Little Ice Age : A period of anomalously cool temperatures observed globally from roughly 1450-1850.

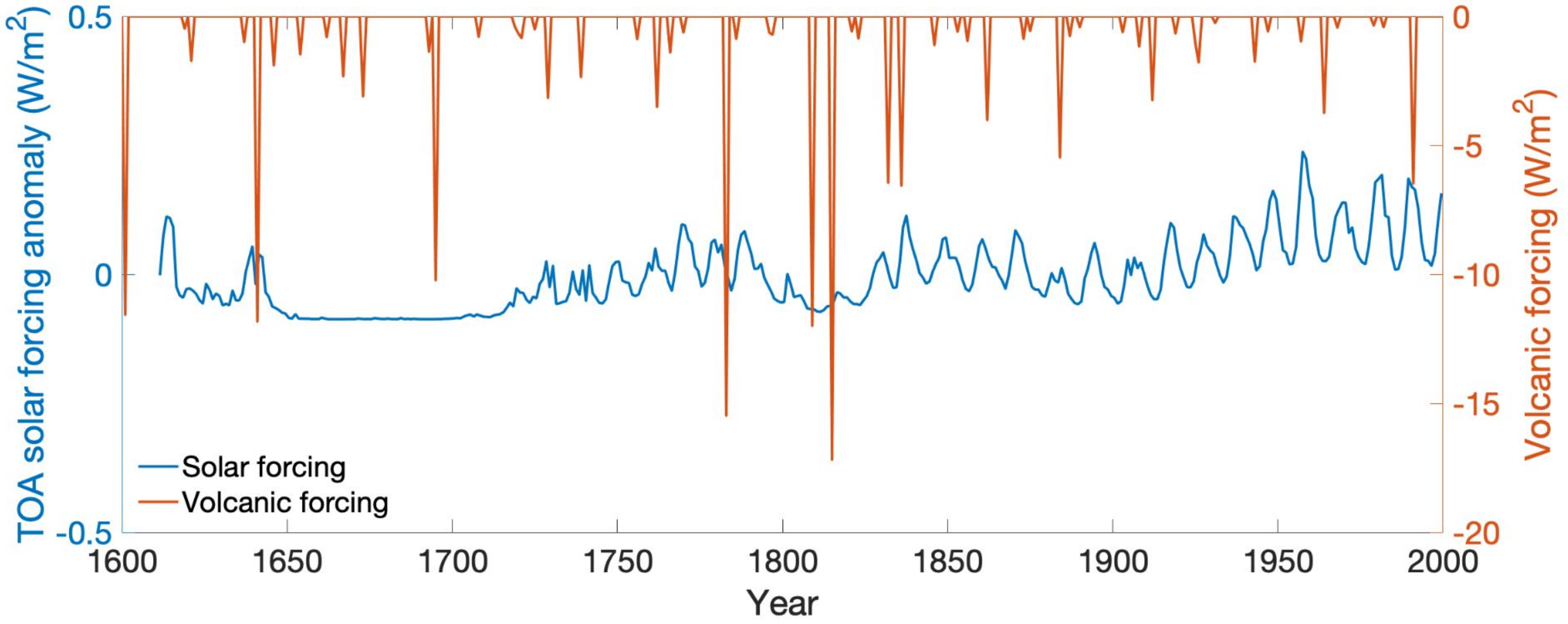

Solar: NRLTSI2 (2015)

Volcanic: Sigl et al. (2015)

Assimilating TSI observations are a challenge

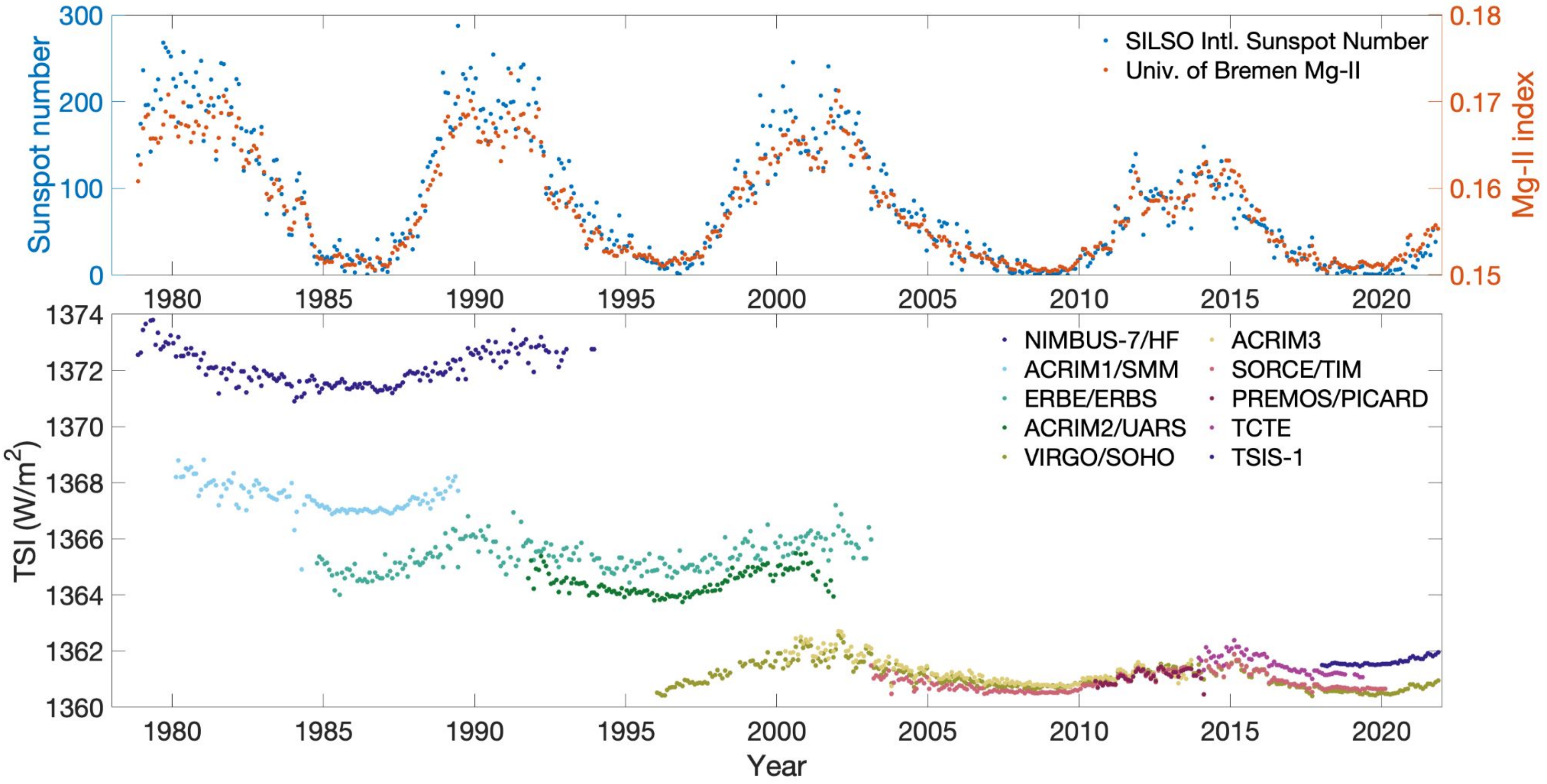

Inferring hidden values from noisy, varied data

- $\mathbf{W}_I$: Instrumental observations
- $\mathbf{T}$: True temperature
- $\mathbf{W}_P$: Proxy observations

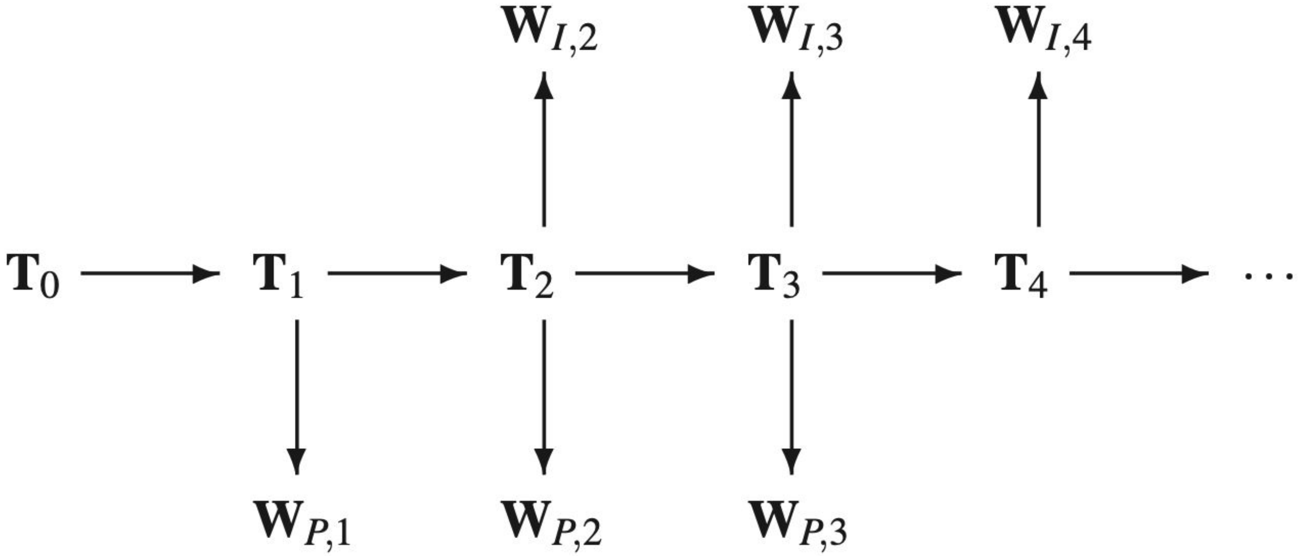

BARSAT schematic for temperature reconstruction (Martin Tingley Thesis)

Proxies as imperfect recorders

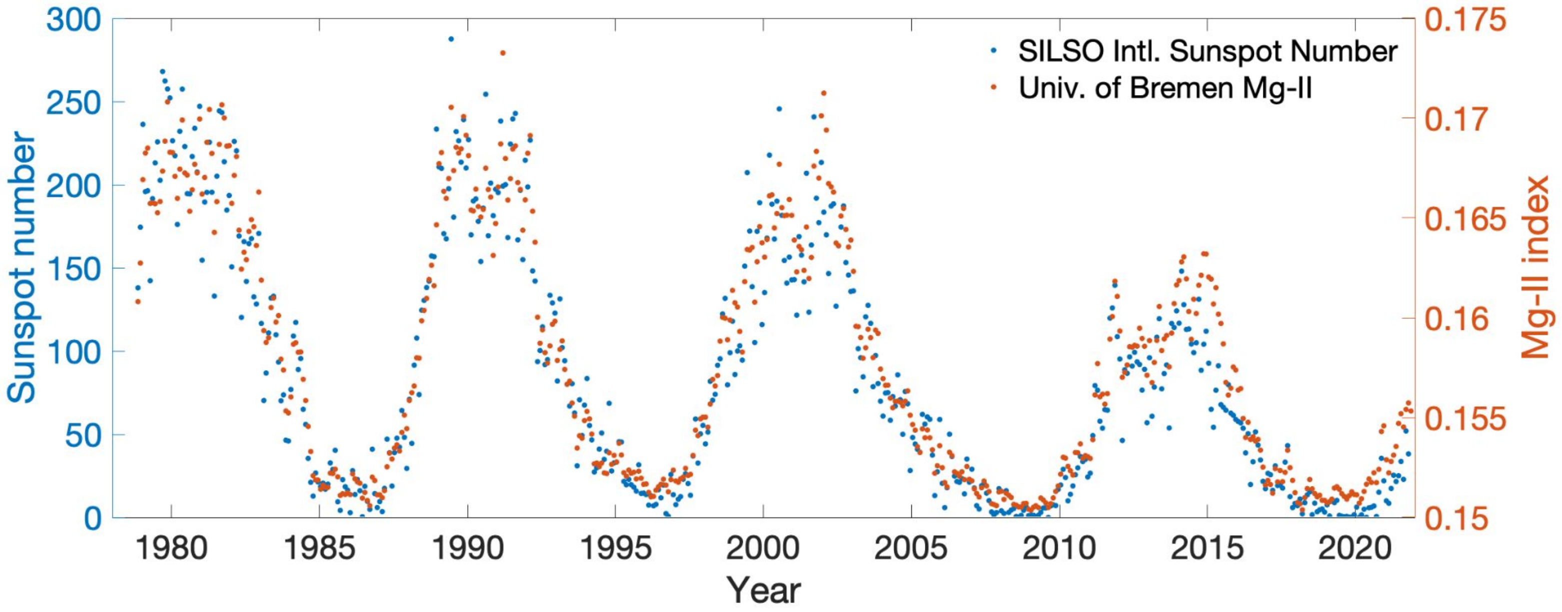

- Proxies are modeled as TSI (x) modified by an inferred offset (a), scaling (b), and uncertainty (ϵ).

$$p_i = a_p + b_p x_i + \epsilon_p$$

Satellites as imperfect recorders

- Satellites are modeled as TSI (x) modified by an inferred offset (a), linear drift (c), and uncertainty (ϵ).

$$s_i = a_s + x_i + c_s t_{i,s} + \epsilon_s$$

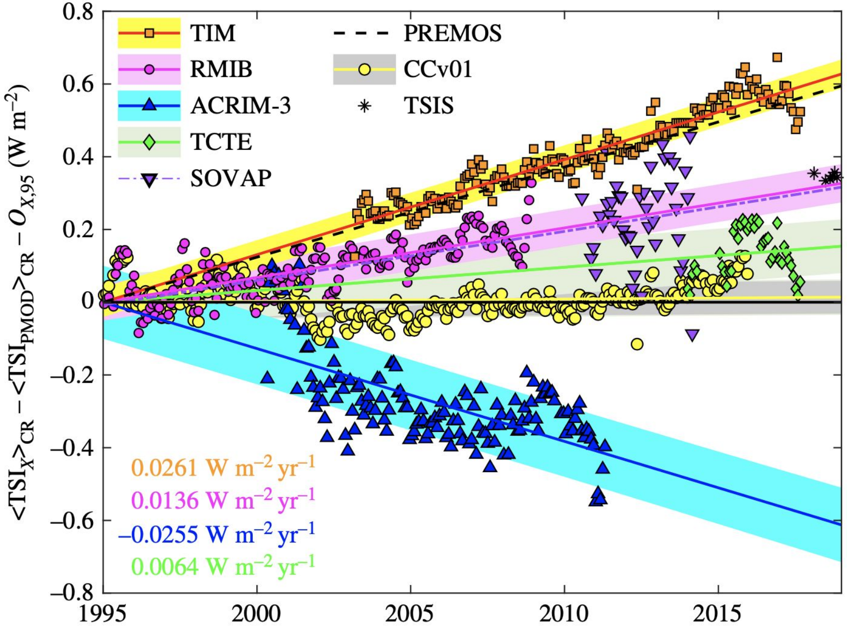

Lockwood and Ball (2020)

Bayesian Kalman filter

We assume that at time i, each contemporaneous observation is an imperfect observation of the true, hidden value of TSI x_i:

$$\underbrace{\begin{bmatrix} s_i \\ p_i \end{bmatrix}}_{\mathbf{y_i}} = \underbrace{\begin{bmatrix} a_s & 1 & c_s \\ a_p & b_p & 0 \end{bmatrix}}_{\mathbf{H}} \underbrace{\begin{bmatrix} 1 \\ x_i \\ t_{i,s} \end{bmatrix}}_{\mathbf{Z}_i} + \begin{bmatrix} \epsilon_s \\ \epsilon_p \end{bmatrix}$$

The true TSI, in turn, is modeled as an AR(2) process updated through a Kalman filter approach:

$$x'_i = \underbrace{\alpha_1 x_{i-1} + \alpha_2 x_{i-2}}_{\hat{x}_i} + \underbrace{\sum_{l=1}^{n_s} K_s \left(s_{i,l} - \hat{s}_{i,l|\hat{x}_i}\right)}_{\text{sat.-based innovation}} + \underbrace{\sum_{m=1}^{n_p} K_p \left(p_{i,m} - \hat{p}_{i,m|\hat{x}_i}\right)}_{\text{proxy-based innovation}}$$

Given the entanglement of the first and second equations, we can numerically solve for these equations through an iterative two-step process of solving for one step while holding the other fixed.

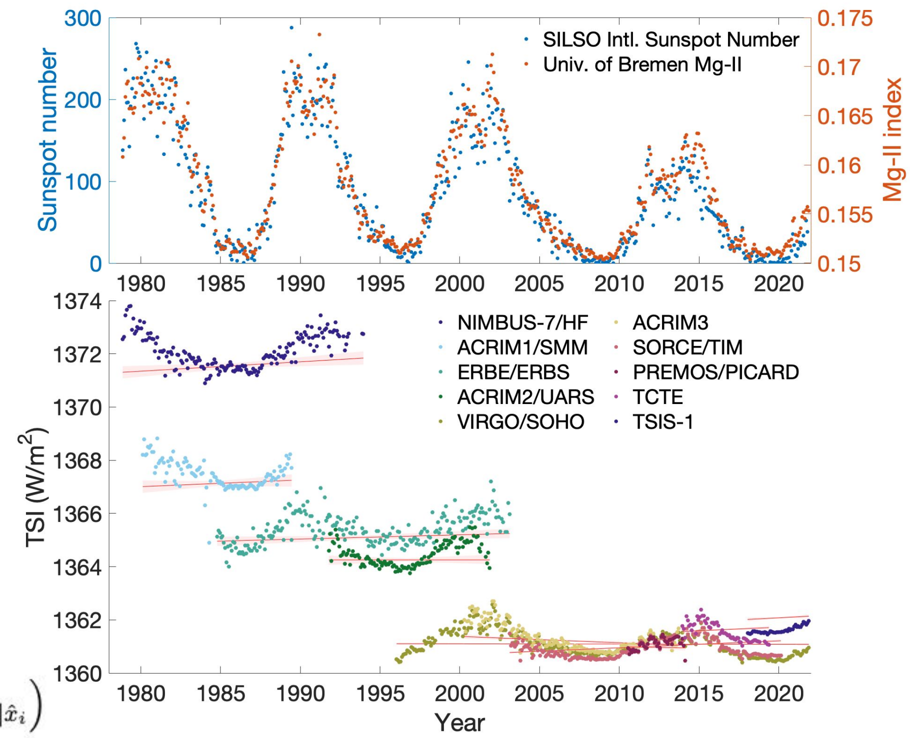

Estimated observer bias structure

Posterior parameter estimates [95% CI]

source	mean anomaly vs SORCE (W/m^2)
Nimbus-7/HF	10.5 [10.4,10.5]
ACRIM1/SMM	6.1 [6.0,6.3]
ERBE/ERBS	4.1 [4.0,4.1]
ACRIM2/UARS	3.3 [3.3,3.4]
VIRGO/SOHO	0.1 [0.1,0.2]
ACRIM3	0.2 [0.2,0.2]
SORCE/TIM	0 (assumed)
PREMOS/PICARD	0.0 [-0.1,0.0]
TCTE	0.6 [0.6,0.6]
TSIS-1	1.1 [1.1,1.1]
Sunspots	—
Mg-II Index	—

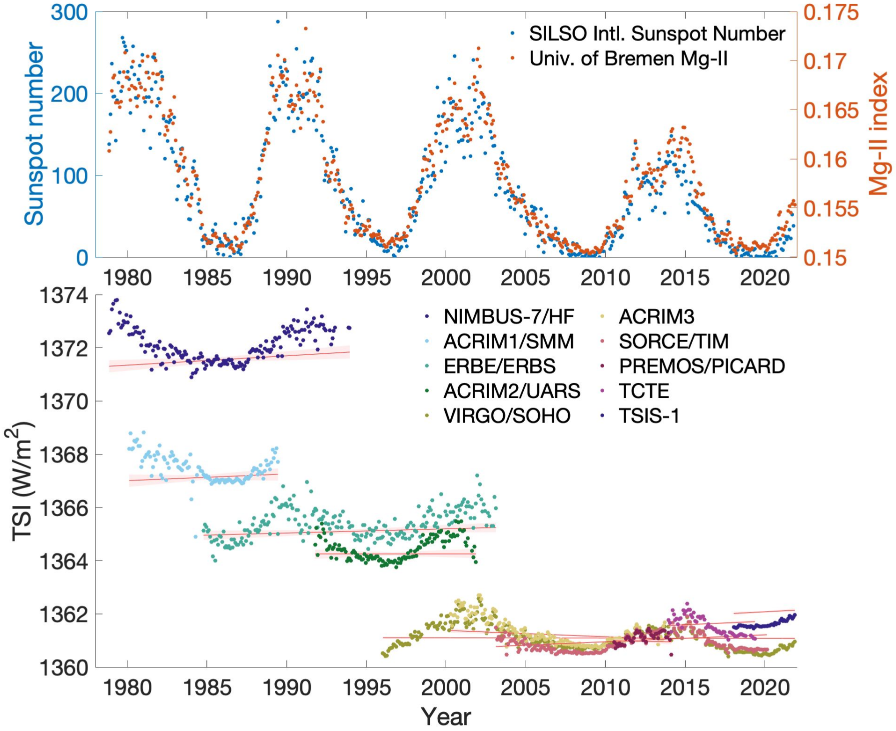

Estimated observer bias structure

Posterior parameter estimates [95% CI]

source	observational uncertainty (W/m^2)
Nimbus-7/HF	0.30 [0.27,0.34]
ACRIM1/SMM	0.32 [0.28,0.36]
ERBE/ERBS	0.31 [0.29,0.34]
ACRIM2/UARS	0.16 [0.14,0.19]
VIRGO/SOHO	0.09 [0.08,0.10]
ACRIM3	0.11 [0.10,0.13]
SORCE/TIM	0.05 [0.04,0.06]
PREMOS/PICARD	0.06 [0.05,0.08]
TCTE	0.06 [0.05,0.08]
TSIS-1	0.02 [0.02,0.03]
Sunspots	0.25 [0.23,0.27]
Mg-II Index	0.20 [0.18,0.22]

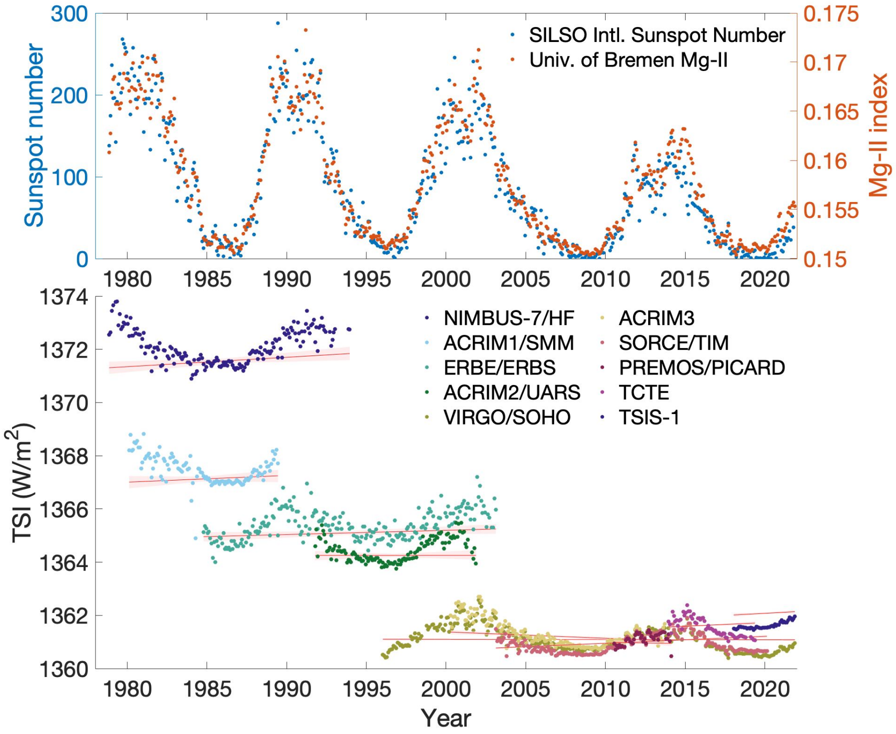

Estimated observer bias structure

Posterior parameter estimates [95% CI]

source	linear drift (W/m^2 per decade)
Nimbus-7/HF	0.37 [0.21,0.52]
ACRIM1/SMM	0.16 [-0.08,0.39]
ERBE/ERBS	0.21 [0.12,0.30]
ACRIM2/UARS	0.08 [-0.06,0.22]
VIRGO/SOHO	-0.05 [-0.08,-0.03]
ACRIM3	-0.23 [-0.29,-0.17]
SORCE/TIM	0.21 [0.17,0.24]
PREMOS/PICARD	-0.02 [-0.25,0.20]
TCTE	0.23 [0.11,0.34]
TSIS-1	0.27 [0.12,0.44]
Sunspots	—
Mg-II Index	—

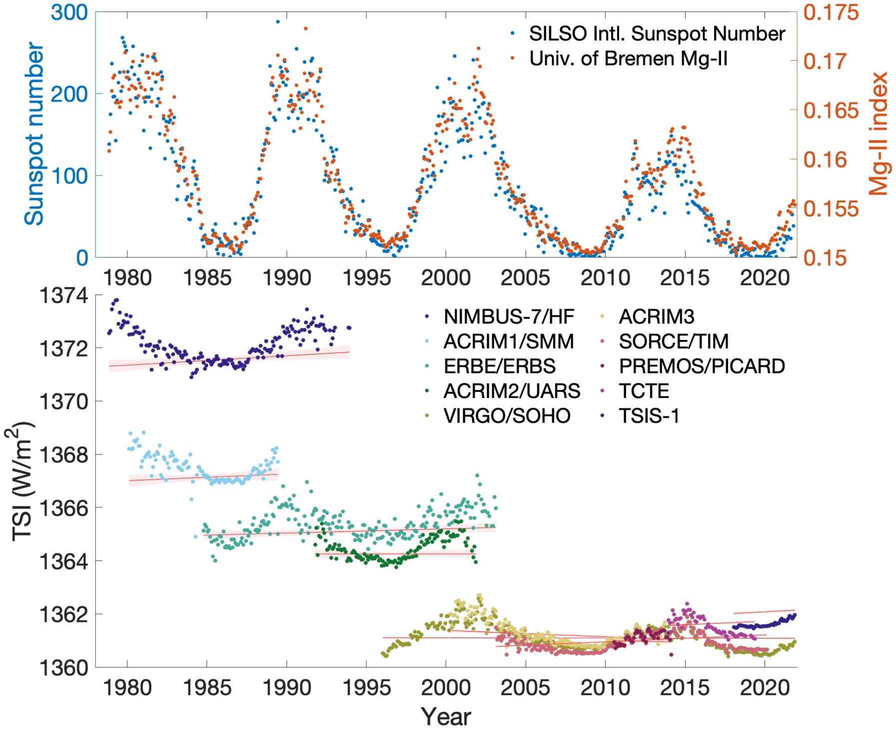

Bayesian TSI reconstruction (BTSI)

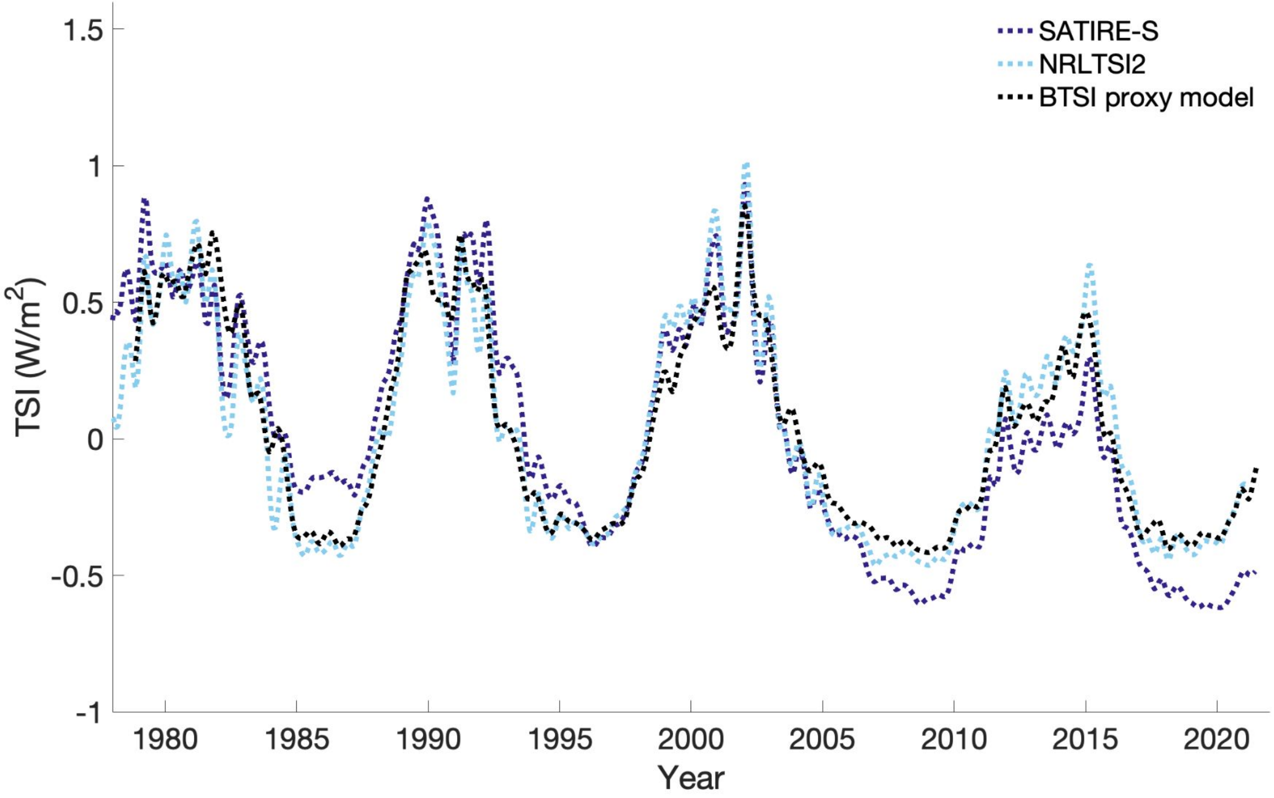

Bayesian TSI reconstruction (BTSI)

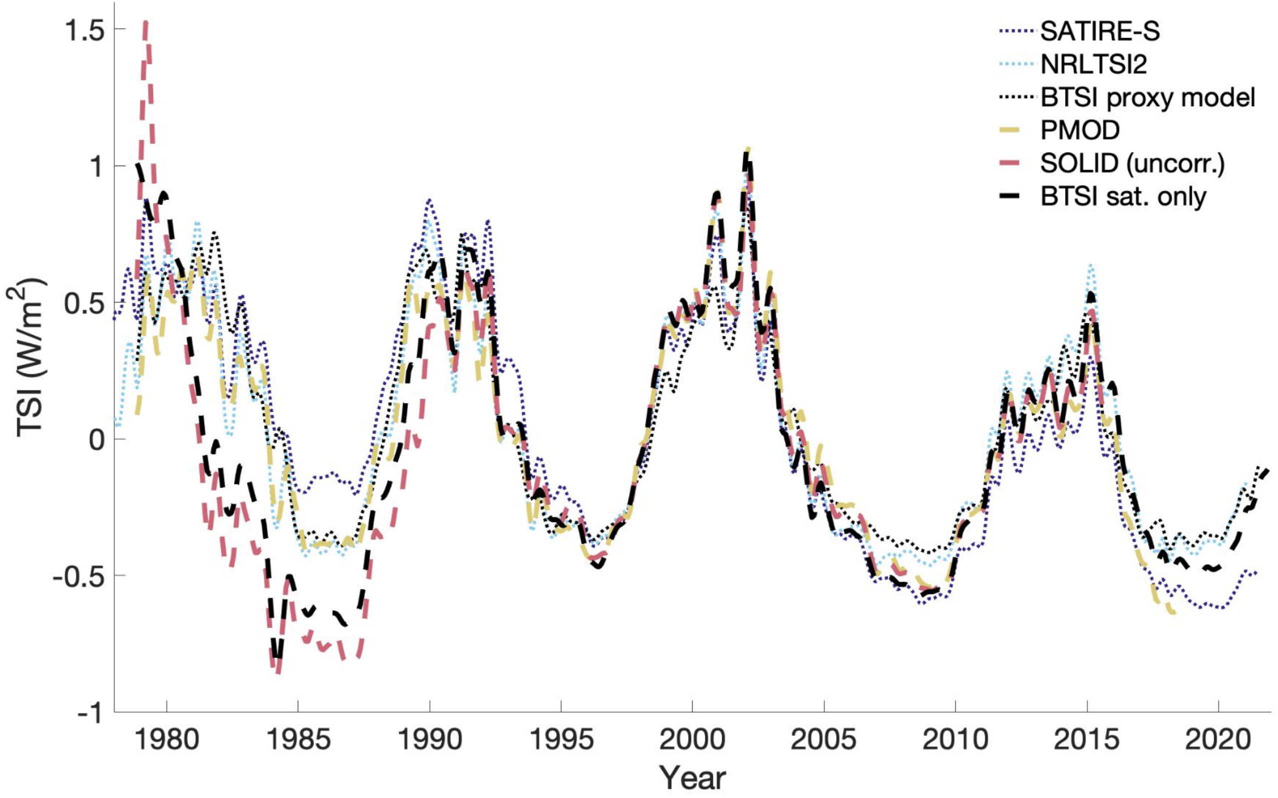

Bayesian TSI reconstruction (BTSI)

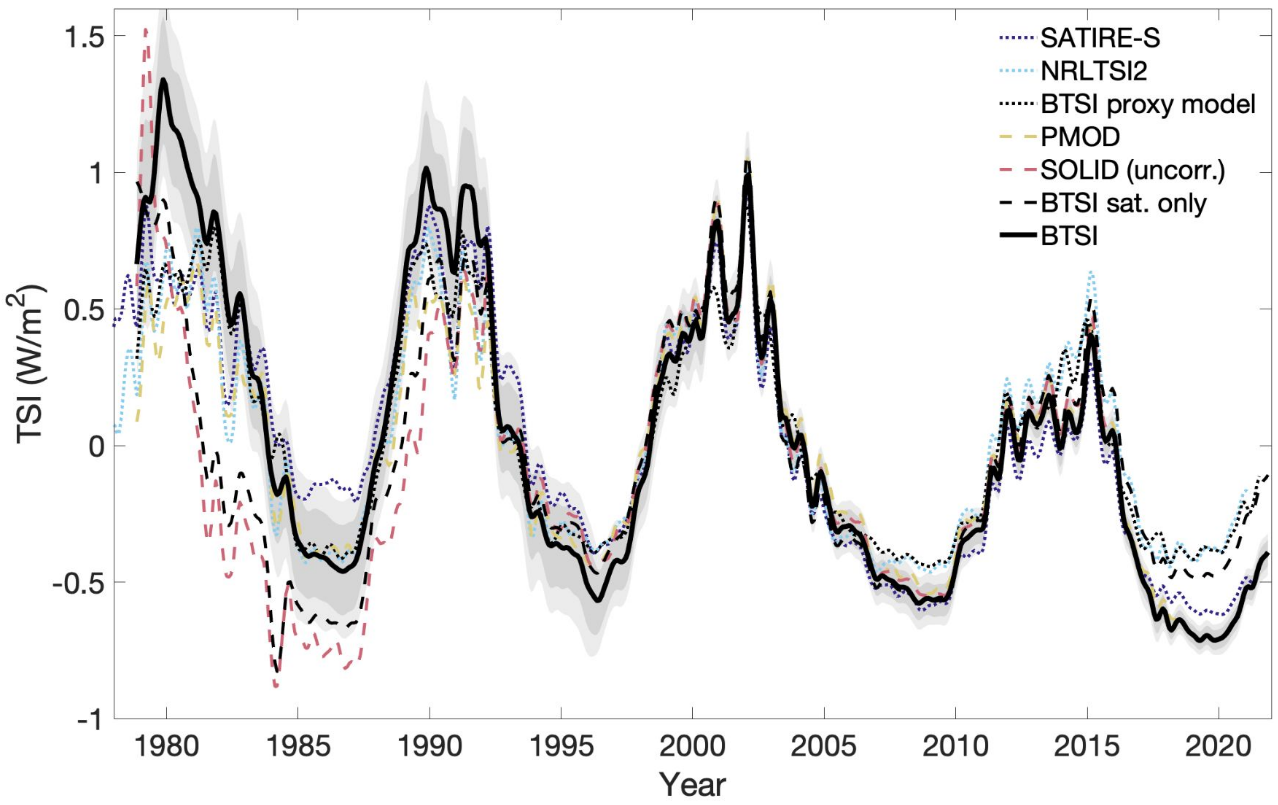

Non-linearity in TSI-proxy relationship

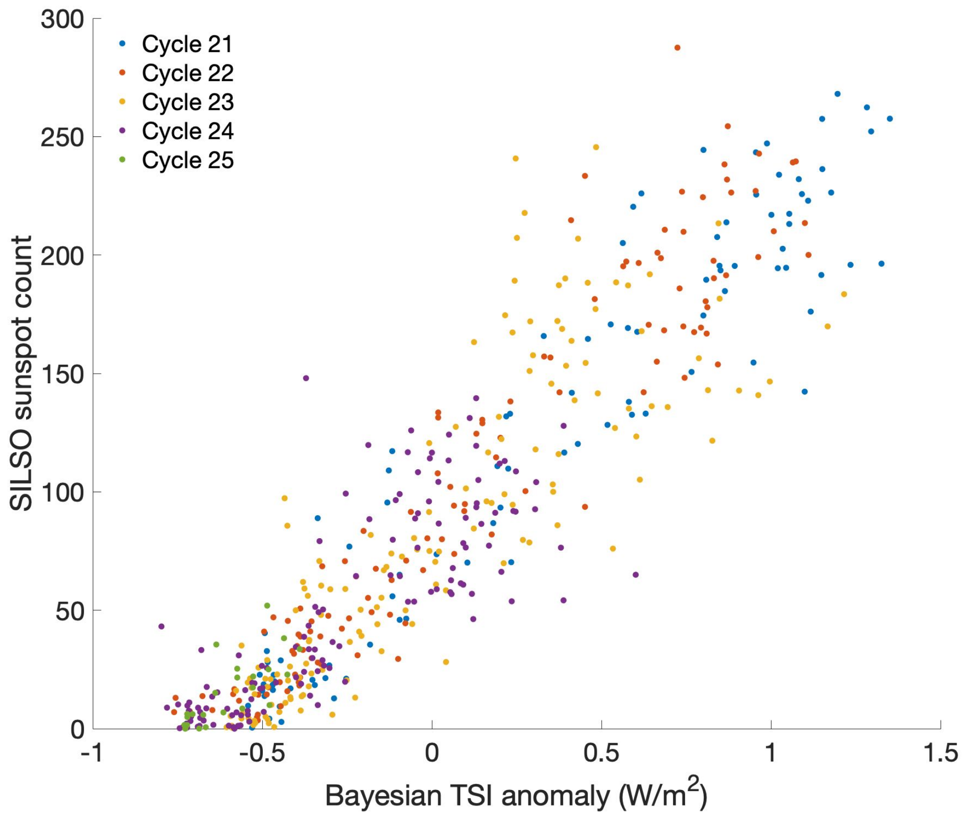

Conclusions

- Both proxies and satellite data can be modeled as imperfect observers with different relative strengths.
- BTSI contains changes in amplitude greater than both satellite-only or proxy-only reconstructions.
- We observe a loss of sensitivity of TSI to magnetic activity proxies at low activity levels.

amdur@g.harvard.edu

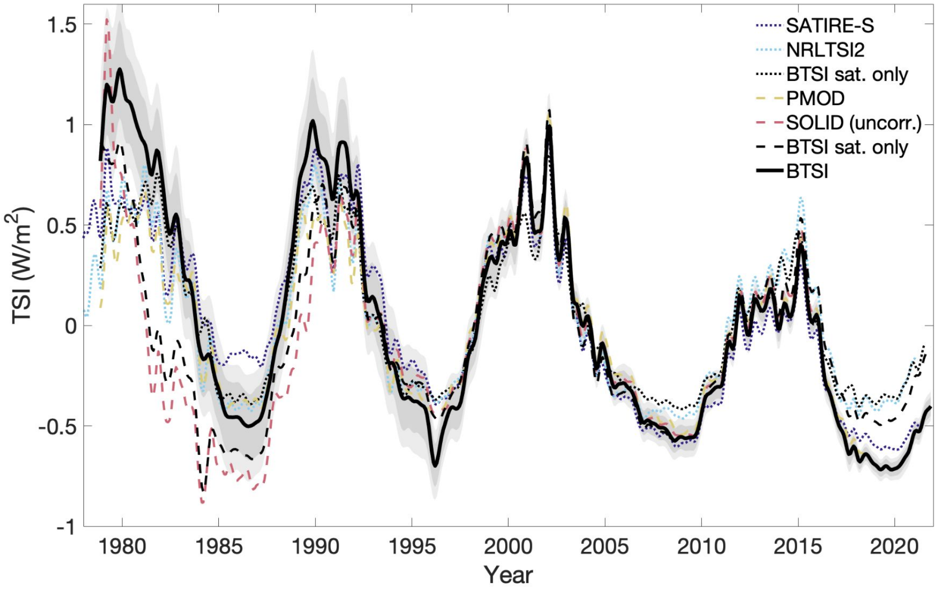

Step 1: Bayesian Regression

$$\underbrace{\begin{bmatrix} s_i \\ p_i \end{bmatrix}}_{\mathbf{y_i}} = \underbrace{\begin{bmatrix} a_s & 1 & c_s \\ a_p & b_p & 0 \end{bmatrix}}_{\mathbf{H}} \underbrace{\begin{bmatrix} 1 \\ x_i \\ t_{i,s} \end{bmatrix}}_{\mathbf{z}_i} + \begin{bmatrix} \epsilon_s \\ \epsilon_p \end{bmatrix}$$

Offsets *a*, TSI-scaling coefficients *b*, instrumental error coefficients *c*, and instrumental noise ϵ are free parameters. *Z* holds the age of the observing instrument, TSI, and a column for the intercept.

Given our priors for the free parameters and a guess for the TSI *X*, we use Gibbs sampling to fit free coefficients in ***H*** to the data ***y*** using multiple regression.

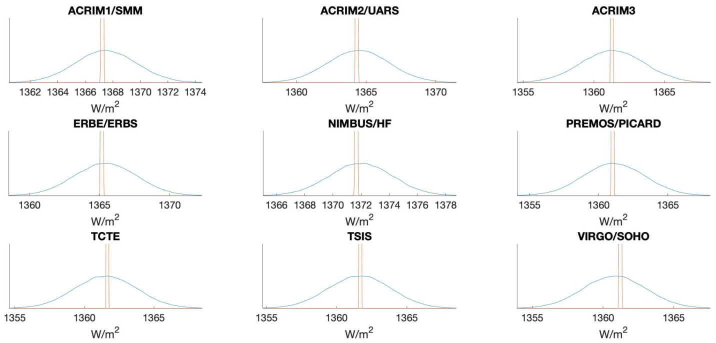

Left: priors (blue) and posteriors (orange) for the satellite offset.
Below: priors (blue) and posteriors (orange) for the linear instrument drift.

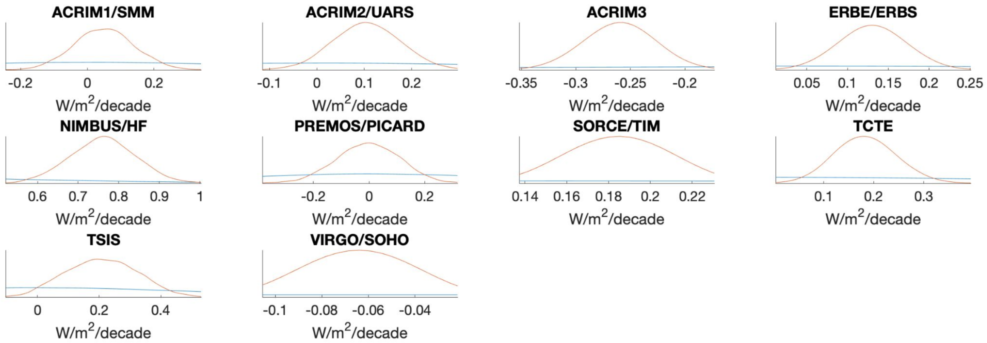

Step 2: Kalman Filter

$$x_i' = \underbrace{\alpha_1 x_{i-1} + \alpha_2 x_{i-2}}_{\hat{x}_i} + \underbrace{\sum_{l=1}^{n_s} K_s \left(s_{i,l} - \hat{s}_{i,l|\hat{x}_i} \right)}_{\text{sat.-based innovation}} + \underbrace{\sum_{m=1}^{n_p} K_p \left(p_{i,m} - \hat{p}_{i,m|\hat{x}_i} \right)}_{\text{proxy-based innovation}}$$

At each time step i, the predicted TSI x_i is updated from $E(x_i)$ using a Kalman Filter, which performs a weighted average of past predictions and observations based upon the estimated accuracy of each source.

Once a full run of the Kalman filter is completed to generate a record of TSI $\boldsymbol{x}$, $\boldsymbol{x}$ is used as a guess to perform Step 1 and generate new estimates for the free parameters $\boldsymbol{H}$ and ϵ.

This recursive loop of **1.** Bayesian regression and **2.** Kalman filtering is repeated until a large sample of estimates is drawn.

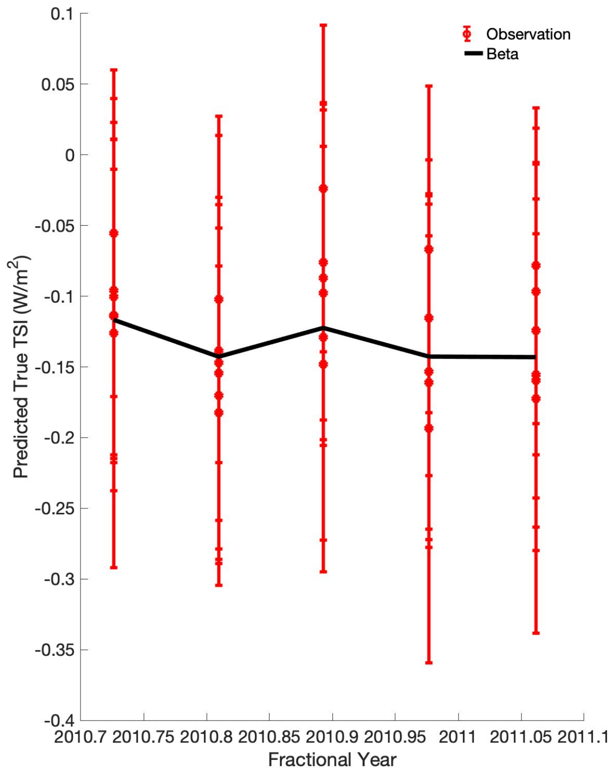

Above: Example of Kalman update for five time steps